Schultz, C.J., S.E. Nelson, L.D. Carey, L. Belanger, B.C. Carcione, C.B. Darden, T. Johnstone, A.L. Molthan, G.J. Jedlovec, E.V. Schultz, C.C. Crowe, and K.R. Knupp, 2012: Dual-polarization tornadic debris signatures Part II: Comparisons and caveats.
Electronic J. Operational Meteor., **13** (10), 138–150.

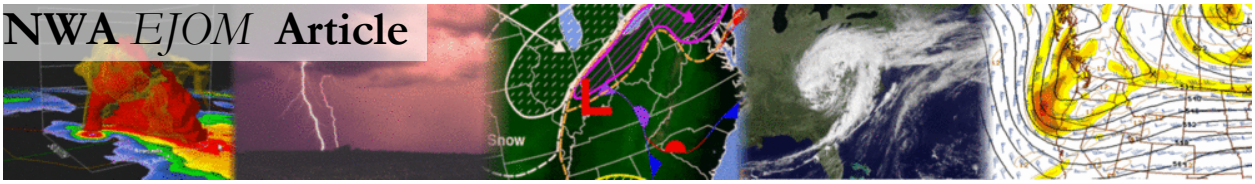

Dual-Polarization Tornadic Debris Signatures Part II: Comparisons and Caveats

CHRISTOPHER. J. SCHULTZ[1, 2], STEVEN E. NELSON[3], LAWRENCE D. CAREY[1], LAURA BELANGER[3], BRIAN C. CARCIONE[4], CHRISTOPHER B. DARDEN[4], THOMAS JOHNSTONE[5], ANDREW L. MOLTHAN[2], GARY J. JEDLOVEC[2], ELISE V. SCHULTZ[1], CHRISTINA C. CROWE[4], KEVIN R. KNUPP[1]

[1]Department of Atmospheric Science, University of Alabama Huntsville, Huntsville, Alabama
[2]NASA Marshall Space Flight Center, Huntsville, Alabama
[3]National Weather Service, Peachtree City, Georgia
[4]National Weather Service, Huntsville, Alabama
[5]National Weather Service, Old Hickory, Tennessee

(Manuscript received 2 March 2012; in final form 23 November 2012)

ABSTRACT

In Part I, several examples of dual-polarization tornadic debris signatures (DPTDS) are presented from multiple tornadic events. Part II's focus is to provide caveats to the DPTDS from operational experience. These examples include a DPTDS in a low signal-to-noise ratio (SNR) region where no damage or falling debris was observed, a case where debris manifested itself after the tornado had lifted, and a third event where DPTDS criteria were met, but no observed damage was found after two storm surveys. Also, low-level displacement of the DPTDS from the ground track is examined, with offsets of 1-4 km from the ground track location. Also discussed was how a higher reflectivity threshold of 30 dBZ could reduce the false detection of debris in the low SNR inflow region of the storm, but could miss weaker DPTDS events. Finally, it is suggested that reflectivity values found within the signature be used as a confidence metric for debris detection when analysis of signatures occur in real-time operations.

1. Introduction

Previous research on dual-polarization tornadic debris signatures (DPTDS) has focused on illustrating examples of the characteristics that the DPTDS signature would exhibit when found within a radar volume (e.g., Ryzhkov et al. 2005, Scharfenberg et al. 2005, Bluestein et al. 2007, Kumjian and Ryzhkov 2008, Carey et al. 2008, Petersen et al. 2008, Snyder et al. 2010, Bodine et al. 2011, Carey et al. 2011, Lemon et al. 2011, Palmer et al. 2011, Schultz et al. 2011,

Corresponding author address: Christopher J. Schultz, NASA Marshall Space Flight Center, 320 Sparkman Dr., Huntsville, AL, 35805
E-mail: christopher.j.schultz@nasa.gov

Bodine et al. 2012, Tanamachi et al. 2012, Schultz et al. 2012, hereafter Part I). Few of these studies have focused on operational applications of the DPTDS, much less any caveats that may exist. As with any new technique or technology, many examples must be collected and analyzed before the community fully understands the strengths and limitations. Thus, the goal of this article is to present caveats of the DPTDS experienced during severe weather situations. These examples provide additional issues to consider when the technique is utilized in day-to-day applications. Proper utilization of the DPTDS will ultimately provide end users with accurate information during severe weather situations.

2. Data collection and polarimetric relation to tornadic debris

Data was collected by the S-band polarimetric Weather Surveillance Radar – 88D at Peachtree City, GA (KFFC; Crum and Alberty 1993, Doviak et al. 2000), and UAHuntsville's Advanced Radar for Meteorological and Operational Research (ARMOR) C-band polarimetric radar located at Huntsville International Airport (Petersen et al. 2007). Both radars gather polarimetric data using a simultaneous H/V technique (slant 45°) and collect reflectivity factor at horizontal polarization (Z_{HH}), radial velocity (Vr), spectrum width (W), differential reflectivity (Z_{DR}), correlation coefficient (ρ_{hv}; also abbreviated CC in Warning Decision Training Branch Modules; WDTB, 2011), and differential phase (ψ_{dp}). Differential propagation phase (Φ_{dp}) is calculated by subtracting radar system offsets, backscatter differential phase, and background noise from ψ_{dp}. Finally, specific differential phase (K_{DP}) is determined by calculating changes in Φ_{dp} over a specific range (e.g., km^{-1}). The volume coverage pattern (VCP; e.g., Brown et al. 2000 a, b) employed for the KFFC events analyzed in this study was VCP 212, and for the ARMOR case, only low-level scanning (0.7º, 1.3º, and 2.0º elevations) was available.

Data from KFFC were analyzed using a combination of the Advanced Weather Interactive Processing System (AWIPS) and the Gibson Ridge Software package GR2Analyst. Data were manually interrogated, and WDTB criteria for detection of tornadic debris at S band were used. These criteria are: evidence a strong differential velocity signature in azimuth supportive of a tornado, $Z_{HH} \geq 20$ dBZ, $\rho_{hv} \leq 0.80$ and $Z_{DR} \approx 0$ dB (WDTB 2011).

Comparisons between the DPTDS and tornado ground track are made through a combination of ARMOR data and satellite information collected by the Moderate Resolution Imaging Spectroradiometer (MODIS; King et al. 1992) on NASA's Aqua and Terra polar orbiting satellites. The MODIS instrument samples in 36 spectral bands and provides the ability to gather information surface vegetation at a resolution of 250 m. Using the red visible channel (620-670 nm), changes in reflectance from vegetation can be determined by differencing MODIS overpasses from before and after the tornado event (e.g., Jedlovec et al. 2006, Carcione et al. 2011, Molthan et al. 2011). NASA's Short-term Prediction Research and Transition (SPoRT) Center at NASA Marshall Space Flight Center (Molthan et al. 2011), utilized overpasses from 17 April 2011 and 4 May 2011 in this differencing technique.

ARMOR data was used to pinpoint the location of the DPTDS. Different from Part I, automated debris detection was employed with more stringent criteria on the radar variables. Each radar pixel was considered part of a DPTDS using the following steps. First, ρ_{hv} was filtered using a 5 gate box car mean. Next, all pixels containing $Z_{HH} \geq 45$ dBZ, a standard deviation of $\psi_{dp} \leq 18$º and $\rho_{hv} < 0.60$ were designated as debris pixels if they were below a height of 1.5 km within a given radar volume. Use of these rigid radar thresholds reduced the chances of false detection of debris due to Mie scatterers like large hail at C band (e.g., Tabary et al.

2009, Anderson et al. 2011, Borowska et al. 2011, Picca and Ryzhkov 2012), as well as, noise, ground clutter and beam filling artifacts. Finally, these pixels were overlaid on the difference imagery created from MODIS in Google Earth to determine distances between the DPTDS and the ground track.

3. Caveats to the DPTDS signature

The purpose of this section is to highlight the care that must be undertaken when analyzing radar data for tornadic debris. Several examples are provided to demonstrate caveats that may arise while using the signature in severe weather situations. These examples are not only applicable to forecasters issuing and verifying severe weather warnings, but are also essential for those who disseminate vital information to the public during these events.

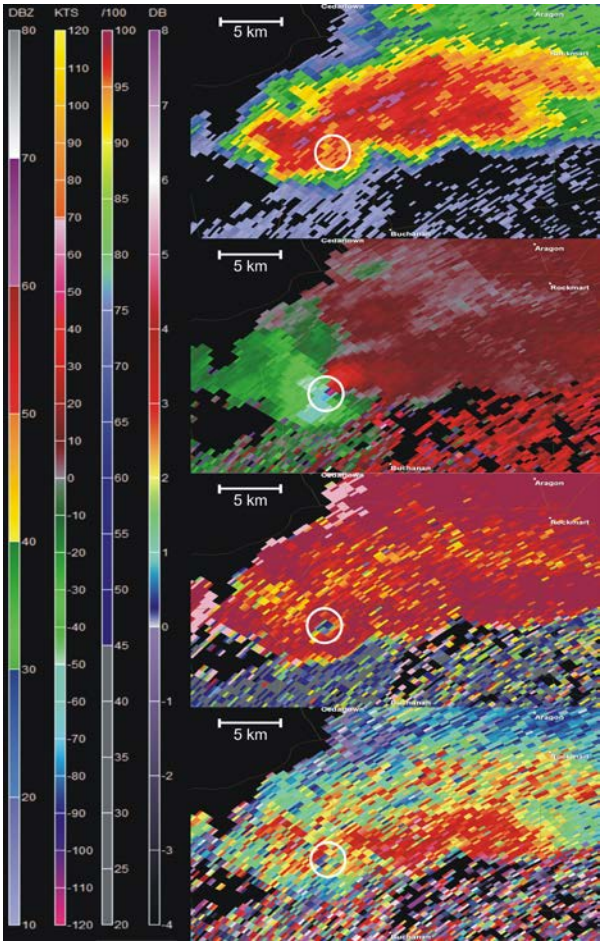

Figure 1. Four-panel image from KFFC on March 2, 2012 at 0114 UTC. Z_{HH} (top panel), V_R (second panel from top), ρ_{hv} (second panel from bottom) and Z_{DR} (lower right) are represented. Scales on the left correspond to Z_{HH} (far left), Vr (middle left), ρ_{hv} (middle right) and Z_{DR} (bottom panel). Z_{DR} has been smoothed to highlight values near 0 dB. White circles indicate the location of the debris signature.

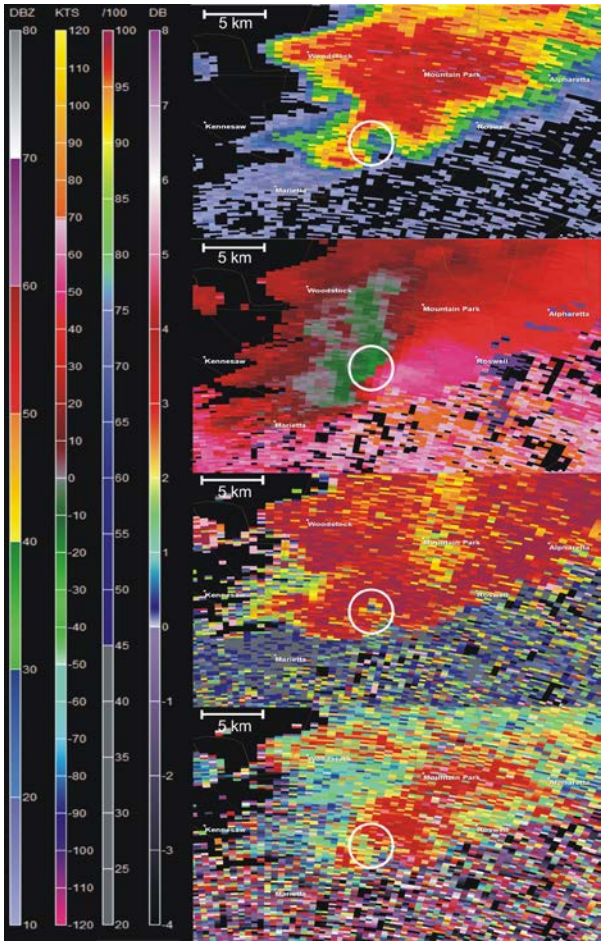

Figure 2. Four panel image from KFFC on March 2, 2012 at 0214 UTC. Panels and scales are the same as Figure 1. White circles indicate the location of the low SNR region misidentified as debris.

a. Low signal-to-noise ratio(SNR) case: 3 March 2012, Haralson and Paulding County, GA

On 3 March 2012 an EF-3 tornado moved across Haralson and Paulding counties in west central Georgia and presented some challenges to NWS meteorologists when determining the existence of tornado debris in polarimetric data. At 0114 UTC, an area of low ρ_{hv} (0.45), a strong differential velocity signature in azimuth in Vr (gate-to-gate velocity difference of 98 m s^{-1}) and high Z_{HH} (50 dBZ) were collocated in the updraft region of a supercell in northern Haralson County from KFFC (Fig. 1). The values of ρ_{hv} and Z_{HH} met WDTB thresholds for a DPTDS for the majority of the time from 0109 UTC through 0147 UTC. However, after 0147 UTC (Fig. 2), the low ρ_{hv} was displaced 2 to 4 km east of the original velocity couplet in an area of lower Z_{HH} (15-25 dBZ vs 35-50 dBZ where previous debris signatures had been located in this storm). During the period between 0146 UTC through 0238 UTC a differential velocity signature in azimuth was present in Vr in this region of lower Z_{HH} and ranged from 28 to 40.1 m s^{-1}. Additionally, a tornadic vortex signature (TVS) was noted in this region of lower Z_{HH} throughout this period. Due to the collocation of low ρ_{hv}, a moderate to strong differential velocity signature, and recent reports of damage likely due to a tornado, meteorologists believed this area of low ρ_{hv} was associated with tornado debris and continued mention of debris in warning products.

A detailed damage assessment was conducted for this tornado the following day. Analysis of the damage path and radar data revealed that for the majority of the tornado's 42 km path, a DPTDS was identified. From the point at which the tornado lifted at 0145 UTC, analysis of the base and polarimetric data showed that the WDTB criteria of the DPTDS were met several times during the next hour. However, no reports of damage or falling debris were received in regions where this signature was observed as it moved through the northern suburbs of Atlanta. It is believed that the low SNR in the inflow region of the storm was the primary reason for the reduction of ρ_{hv}.

b. Scanning strategy and lingering debris: 22 December 2011, Moreland, GA

Scanning strategy plays a large role in how quickly debris can be discerned in a radar volume. Such was the case as a quasi-linear convective system (QLCS) produced several short-lived tornadoes in the NWS Peachtree City County Warning Area on December 22, 2011. Examining the radar volume at 2244 UTC from KFFC in Figure 3, no readily discernible debris signature was present in ρ_{hv} in the 0.5º elevation scan; however a velocity signature in azimuth was present in Vr (33 m s^{-1}; 36 m s^{-1} inbound and 3 m s^{-1} inbound, separated by 1.0 km). At the next volume scan time (2248 UTC) a small debris signature was present near Moreland, GA. At this time ρ_{hv} dips to 0.67, Z_{DR} drops as low as -2.1 dB, Z_{HH} is approximately 46 dBZ and the weakening circulation (24.5 m s^{-1}, separated by 0.40 km) was collocated with the lowering in both ρ_{hv}, Z_{DR}, and Z_{HH} (Fig. 4). Also, this signature had vertical extent to about 0.75 km (or 2.4 degrees in VCP 212). According to ground survey information, this short-lived tornado touched down at approximately 2244 UTC, lifted by 2246 UTC, and was on the ground for only 3 km, so the DPTDS was observed at 0.5º elevation *after* the tornado has lifted. Examining subsequent radar volumes at 2253 and 2258 UTC, lofted debris was still present in the radar volume as it settled to the surface (Figs. 5 and 6); however, no discernible velocity signature/couplet was evident in the region of lowered ρ_{hv}. One should notice how the debris had fanned out in space when compared to Figure 3 and many of the other examples presented in

Part I. While the debris was not concentrated, many pixels still met the Z_{HH} and ρ_{hv} thresholds for debris (>20 dBZ and < 0.80), and Z_{DR} was predominately negative, ranging from -3.0 dB to 1 dB during this period. Beyond 2258 UTC the signature was not clearly seen. This phenomenon has also been observed in Lemon et al. (2011) and Bodine et al. (2012).

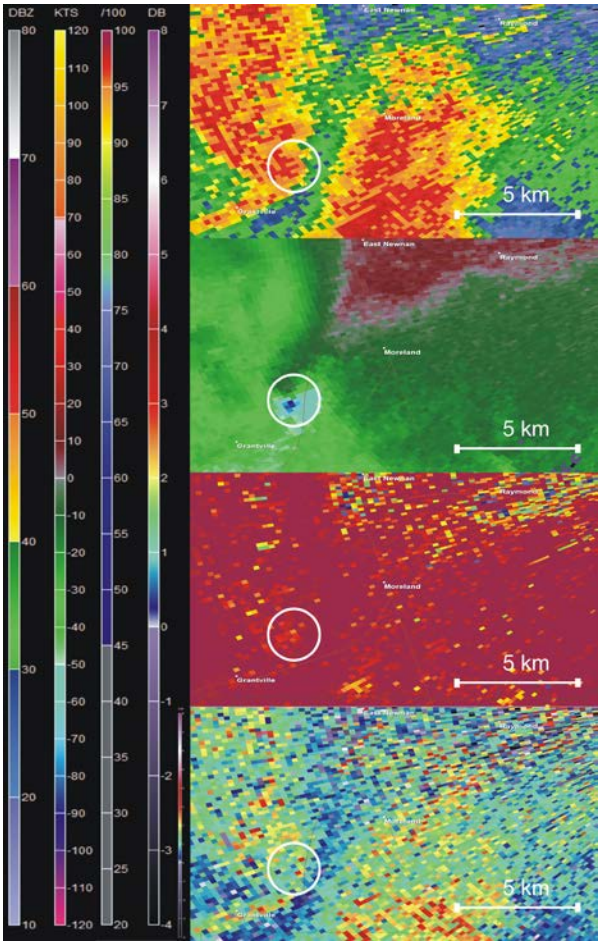

Figure 3. Four panel image at 2244 UTC on December 22, 2011, from the WSR-88D radar KFFC at 0.5 degrees elevation and at a range of 25 km. Color scales are the same as Figure 1.

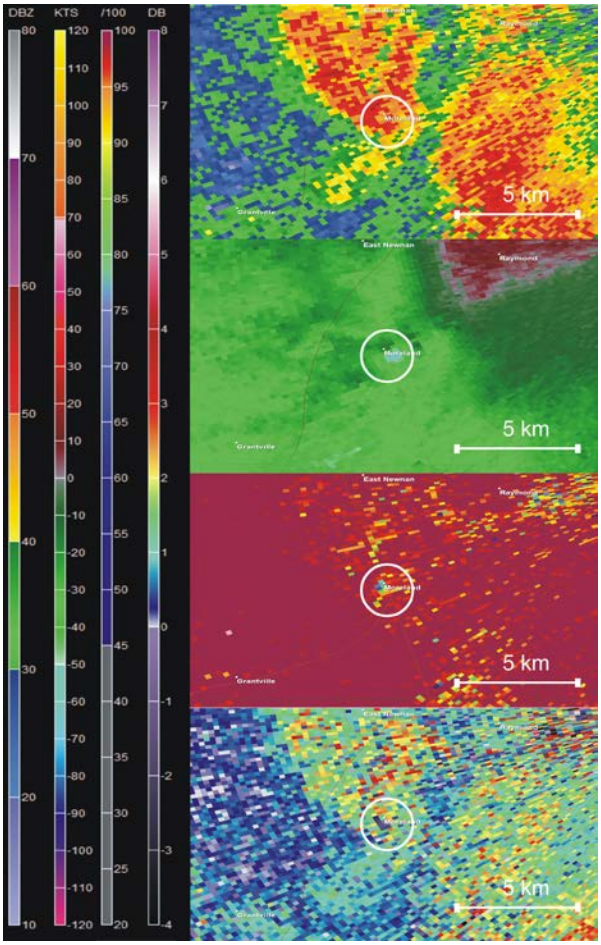

Figure 4. Four panel image at 2248 UTC on December 22, 2011, from the WSR-88D radar KFFC at 0.5 degrees elevation and a range of 20 km. Image information is the same as Figure 3.

c. DPTDS location versus ground track location: Hackleburg-Tanner-Harvest, AL, tornadoes, 27 April 2011

In situations where DPTDS events are clear cut (i.e., a large area of debris in ρ_{hv}) it is still important to distinguish between tornado debris and ground location when exploiting the DPTDS during severe weather situations. Figure 7 examines the MODIS satellite-derived tornado track and DPTDS location of the long track Hackleburg, AL, EF-5 tornado near the towns of Hillsboro and Harvest, AL. Most of the DPTDS boxes align quite well with the ground track location and are within 1 km of the damage path. However, one can also see a few instances in this figure where there is some displacement between the track and radar observed signature that are greater than 1 km. Similar observations are made in the lower panel of Figure 7 near Harvest, AL. Displacement of the debris signature from the ground track has been observed in other studies

(e.g., Magsig and Snow 1998, Carey et al. 2008, Carey et al. 2011, Palmer et al. 2011), and has been seen as far as 4 km from the track. Therefore, as the meteorological community exploits "street-level" information in severe weather coverage, uncertainty still needs to be conveyed when discussing the exact location of a tornado during events, even with such a strong indicator like the tornadic debris signature.

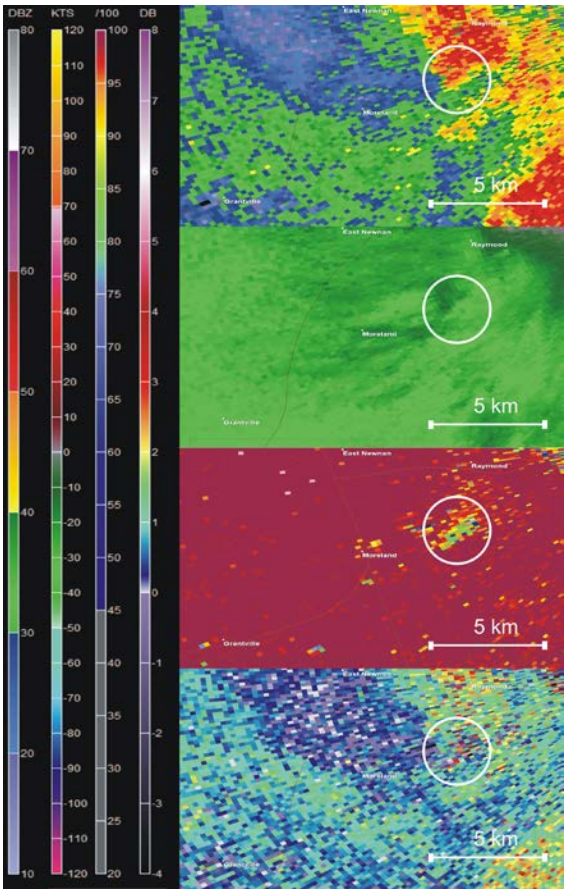

Figure 5. Four panel image at 2253 UTC on December 22, 2011, from the WSR-88D radar KFFC at 0.5 degrees elevation and at a range of 15 km. Image information is the same as Figure 3 except that circles denote the area where lofted debris is still present.

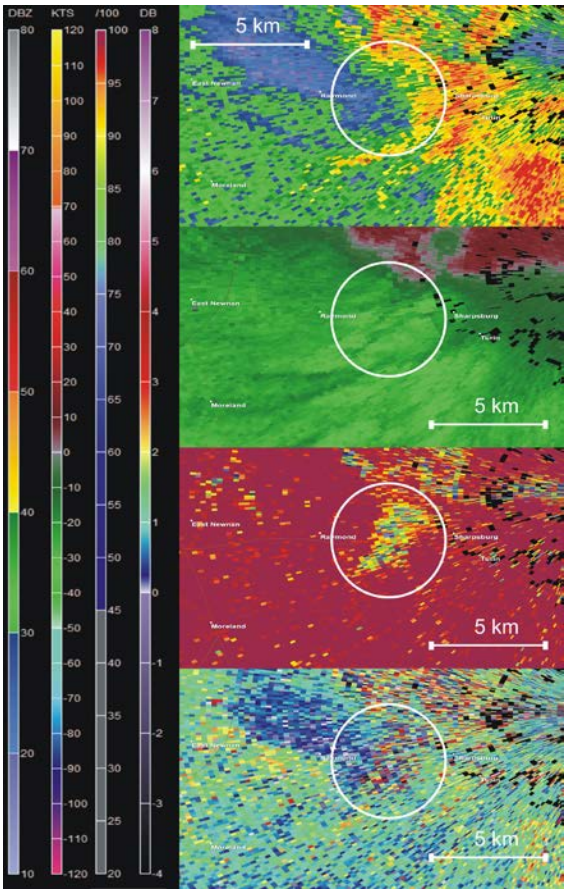

Figure 6. Four panel image at 2258 UTC on December 22, 2011, from the WSR-88D radar KFFC at 0.5 degrees elevation and a range of 10 km. Image information is the same as Figure 5.

d. DPTDS but no damage found: 21 January, 2012, Coweta County, GA

Another challenging event occurred 9.3 km to the southwest the KFFC radar as a QLCS moved across Coweta County on January 21, 2012. The QLCS produced an EF-1 tornado about 3.7 km northeast of Moreland, GA (same town as part 3*a.*, but a different event) around 1710 UTC and an isolated area of wind damage near Senoia, GA (about 18 km east of Moreland) around 1731 UTC. However, analysis of the polarimetric data for this event showed at least two DPTDSs. One DPTDS was seen at 1713 UTC, associated with the Moreland tornado, another was observed 2.8 km south of Turin, GA around 1721 UTC (Figs. 8 and 9). The second DPTDS

was the more interesting of the two. A distinct area of very low ρ_{hv} (≤ 0.35) was collocated with a velocity signature in azimuth in Vr (27 m s^{-1}; 22.6 m s^{-1} inbound, 4.5 m s^{-1} outbound, separated by 0.30 km) and high Z_{HH} (> 50 dBZ) was seen (Fig. 9). This signature also contained vertical continuity, as it was seen collocated with the differential velocity signature in Vr up to 1.3° elevation (~180 m AGL). However, local officials reported no damage in this area as did the initial NWS damage assessment survey. A second survey was conducted a month later and again found no visible damage.

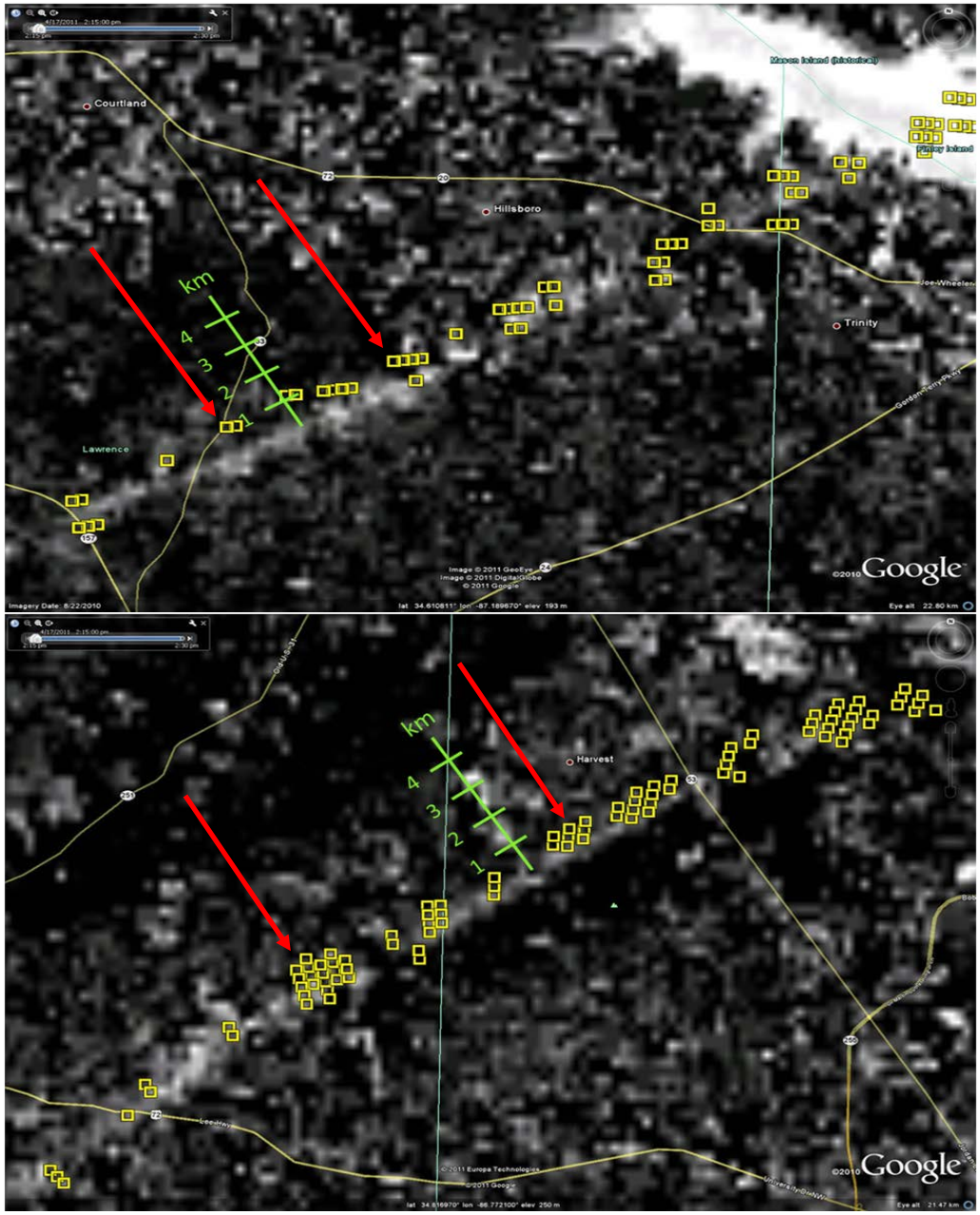

Figure 7. MODIS Channel 1 (620-670 nm) difference image with low level ARMOR DPTDS information overlaid (yellow boxes) for the Hackleburg-Tanner-Harvest EF-5 tornado. MODIS imagery was taken from Aqua MODIS on 17 April 2011 and Terra MODIS on 4 May 2011. The top panel is a section of the track near Moulton AL, and the bottom panel is a section of the track near Harvest, AL. Red arrows highlight where the displacement is most evident.

Unlike the 3 March 2012 event (Section 3*a*.) Z_{HH} was much higher (46 dBZ vs $\leq$ 25 dBZ) and this signature was not located in the low SNR inflow region of the storm. It is speculated that the vortex apparent in Vr with the second DPTDS did not extend fully to the surface or was not strong enough to produce visible damage to trees or structures. Even with sub-tornadic wind speeds at the surface with this vortex the wind speed and updraft may have been strong enough to loft light debris such as pine needles high enough to be detected by the radar. The range to this location from the radar is about 7.8 km and the altitude of the center of the 0.5° beam at this range is approximately 60 m AGL.

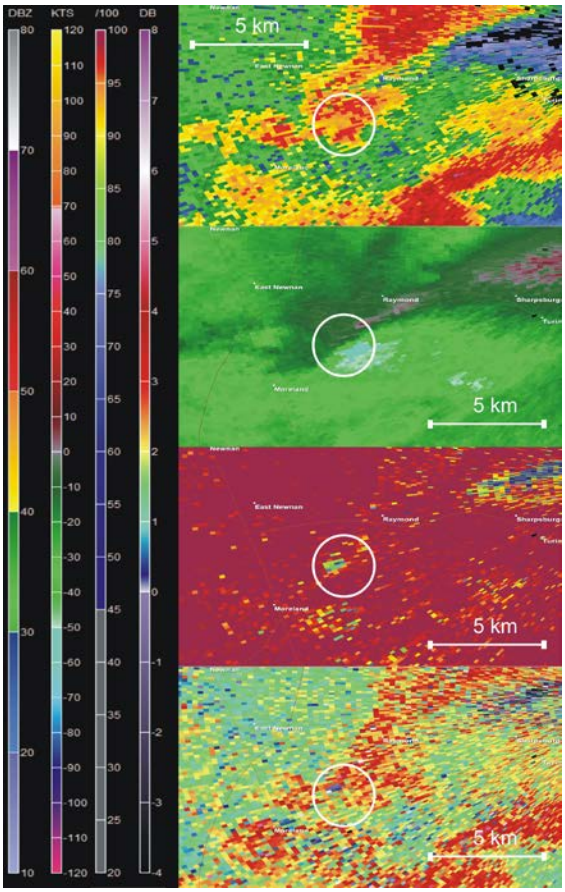

Figure 8. Four panel image from KFFC on January 21, 2012 at 1712 UTC. Panels and scales are the same as Figure 1. White circles indicate the location of the DPTDS.

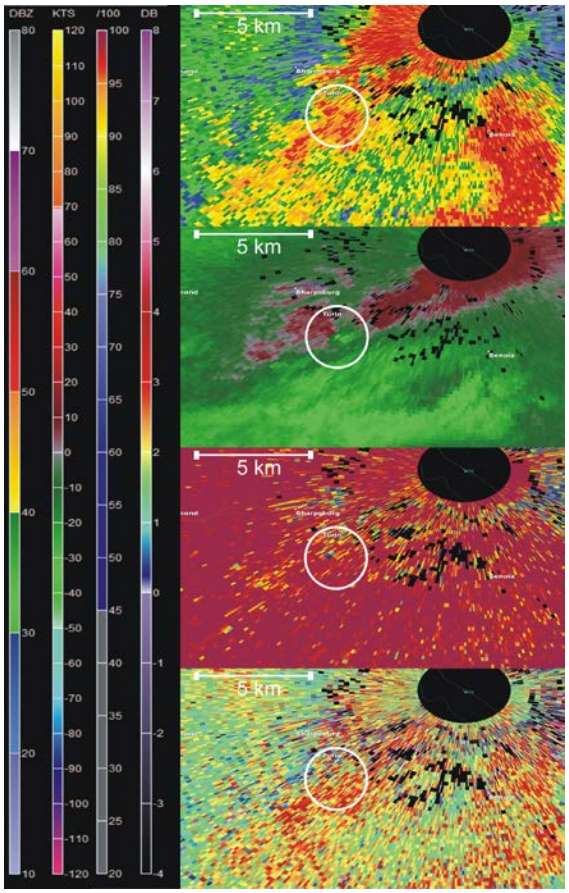

Figure 9. Four panel image from KFFC on January 21, 2012 at 1721 UTC. Panels and scales are the same as Figure 1. White circles indicate the location of the DPTDS.

4. Discussion

Operational application of the DPTDS will likely become a key aspect of situational awareness during tornadic events as the implementation of dual-polarization technology moves forward in the coming years. While fundamental concepts have been outlined in the literature toward the application of polarimetric information to the detection of tornadic debris, it still remains a work in progress as how to best implement these concepts as procedures for the warning decision-making process. Namely, with the ever increasing amount of information that

an operational forecaster may have to sift through during a hazardous weather event (radar, satellite, models), the question remains: "Will the forecaster have enough time to explore all of the data at hand, and make the correct decision?" Situations will vary among offices and events based on the number of staff available and the expansiveness of the event, and there may be situations where a forecaster could have the time to perform detailed radar analysis.

An automated DPTDS algorithm similar to the one employed in Section *3c.* could be part of the solution to the questions posed above for operational implementation of the signature. However, there are a few things that need to be addressed before such implementation is possible. First, a large sample set of storms is needed to test any algorithm on a variety of cases. This sample size needs to cover a variety of event types and include cases where false detections are possible and this sample should be much larger than those found in previous studies (e.g., Part I, Bodine et al. 2012). Also, this algorithm should be transparent, so the end user understands why a particular region of a storm has been highlighted for debris. This would especially be important for false detections that might occur with any automated algorithm. Most importantly, the raw radar data needs to still be available for the end user to further investigate any detected signature, if warranted.

As indicated in Section 3*a.*, there will be times where using simple thresholds can still provide false alarms on debris detection. That particular signature met all of the WDTB criteria: there was a TVS collocated with several pixels in the 20-25 dBZ range in Z_{HH}, ρ_{hv} dropped significantly (as low as 0.26), and Z_{DR} was as low as -1.8 dB. Using the criteria from Ryzhkov et al. (2005) or Part I; however, this signature would not have reached the Z_{HH} threshold for debris. Use of a higher Z_{HH} threshold such as 30 dBZ should reduce false detection of debris within the low SNR inflow region of storms like the one examined in Section 3a. However, it may also miss weaker debris signatures in regions with the lower reflectivity threshold of 20 dBZ. Therefore, it is advantageous to use reflectivity as a measure of confidence in polarimetric debris detection. Thus, confidence that a particular signature is debris increases as reflectivity within the signature increases if all other criteria for radar derived debris are met. Again, no specific threshold is perfect (as shown here and in Bodine et al. 2012) and it should be emphasized that the use traditional methods for tornado detection must be used first before searching for debris (e.g., WDTB 2011, Schlatter 2012).

On the other hand, damage may not always be found with all DPTDS events. Unlike the example in Section 3*a.*, the DPTDS in Section *3d.* met all proposed thresholds (WDTB, Ryzhkov et al. 2005, Part I) and damage was not found after two damage surveys. Thus, the presence of this signature will provide increased confidence that a tornado may be present, but will not always provide confirmation of damage until a ground survey can be completed.

Pinpointing the location of a tornado threat is important, but as demonstrated above it is unlikely that one can give the exact street-by-street location of the tornado's ground track using the DPTDS due to the observed displacement between the DPTDS and the actual ground track location. This is especially important because people have been found to use specific cross-streets or locations as frames of reference to determine if they should take shelter (Klockow et al. 2012). The results presented above echo the same fundamental ideas. The DPTDS can narrow down the areal scope of a warning, say to a section of town or a county, but it is not suggested that this signature be used to give street-by-street warning because the tornado could be a few kilometers away from the location of the DPTDS on radar. Importantly, usage of common landmarks for frames of reference for those in the path of the storm should not be abandoned, as it has been shown to be useful to many in post event surveys (K. Klockow, personal

communication, 2012). However, some uncertainty should be conveyed when trying to highlight potential tornadic activity within a section of a town or county given the offset observed between ground location and DPTDS signature seen above. A good example of the use of the DPTDS during a tornado event is from WRAL-TV's coverage of the April 16, 2011 tornado event near Raleigh, NC (Johnson 2011[1]).

5. Conclusions

Presented above were important comparisons and caveats from operational experience with the DPTDS. Highlighted was an event where WDTB's criteria for a DPTDS were observed in the inflow region of a previously tornadic supercell storm, and no damage or debris was found near the location of the DPTDS. Also presented was a case where the tornadic debris manifested itself in the radar volume after the tornado had lifted in a short-lived event. Comparisons were made between ground track locations and DPTDS events in two cases. These comparisons revealed that the DPTDS at low levels (< 1.5 km) was 1-4 km to the left of the tornado track and was consistent with previous work on offsets between velocity couplet location and tornado track. Finally, presented was an example where a DPTDS was observed, but no damage was found after an extensive storm survey. It is important to remember that this signature is only useful once the tornado has touched down. Thus, it is also important to examine the polarimetric data for clues then can add confidence to accurately warn on an impending tornado event (e.g., Kumjian and Ryzhkov 2008, Crowe et al. 2010, Kumjian 2011, Crowe et al. 2012).

Acknowledgements. Thank you to Paul Schlatter and James LaDue for additional discussion of DPTDSs at S-band; particularly with the January 21, 2012 DPTDS no damage case. Results and discussion from post event surveys of people who were directly affected by tornadoes were graciously provided by Kim Klockow, and are much appreciated by the authors, in order to provide insight into how the public reacts to the warning process. UAHuntsville co-authors wish to acknowledge support from NOAA Grant NA090AR4600204. C. Schultz would also like to acknowledge additional support through the NASA Cooperative Education Program at NASA Marshall Space Flight Center. Finally, the authors wish to acknowledge the two anonymous reviewers who provided constructive criticism and helped shape the final version of this article.

REFERENCES

Anderson, M., L. D. Carey, W. A. Petersen, and K. R. Knupp, 2011: C-band dual-polarimetric radar signatures of hail. *Electronic J. Operational Meteor.*, **12** (2), 45-75.

Bluestein, H. B., M. M. French, R. L. Tanamachi, S. Frasier, K. Hardwick, F. Junyent, and A. L. Pazmany, 2007: Close-range observations of tornadoes in supercells made with a dual-polarization, X-band, mobile Doppler radar. *Mon. Wea. Rev.*, **135**, 1522–1543. doi: 10.1175/MWR3349.1

[1] To see this coverage, visit http://www.wral.com/news/video/9452204/ and watch from 00:50:00 through 00:53:00.

Bodine, D., M. R. Kumjian, A. J. Smith, R. D. Palmer A. V. Ryzhkov, and P. L. Heinselman, 2011: High resolution polarimetric observations of an EF-4 tornado on 10 May 2010 from OU-PRIME. *35th Conf. on Radar Meteorology*, Pittsburgh, PA, Amer. Metor. Soc.

Bodine, D. J., M. R. Kumjian, R. D. Palmer, P. L. Heinselman, and A. V. Ryzhkov, 2012: Tornado damage estimation using polarimetric radar. *Wea. and Forecasting*, in press. doi: 10.1175/WAF-D-11-00158.1

Borowska, L., A. Ryzhkov, D. Zrnić, C. Simmer, and R. Palmer, 2011: Attenuation and differential attenuation of 5-cm-wavelength radiation in melting hail. *J. Appl. Meteor. Climatol.*, **50**, 59–76. doi: 10.1175/2010JAMC2465.1

Brown, R. A., J. M. Janish, and V.T. Wood, 2000a: Impact of WSR-88D scanning strategies on severe storm algorithms. *Wea. Forecasting*, **15**, 90–102.

———, V. T. Wood, and D. Sirmans, 2000b: Improved WSR-88D scanning strategies for convective storms. *Wea. Forecasting*, **15**, 208–220.

Carcione, B. C., K. B. Laws, G. J. Jedlovec, A. Molthan, M. Smith, and F. LaFontaine, 2011: Use of NASA satellite data in tornado damage path assessment. *36th Annual NWA Conference*, Birmingham, AL, Natl. Wea. Assoc.

Carey, L.D., W. A. Petersen, and K. R. Knupp, 2008: ARMOR dual-polarimetric radar observations of two tornadic supercells during the 2008 Super-Tuesday tornado outbreak. *33rd NWA Annual Meeting*, Louisville, KY, Natl. Wea. Assoc.

———, and Coauthors, 2011: Dual-polarimetric radar-based tornado debris paths associated with EF-4 and EF-5 tornadoes over Northern Alabama during the historic outbreak of 27 April 2011. *36th Annual NWA Conference*, Birmingham, AL, Natl. Wea. Assoc.

Crowe, C. C., C. J. Schultz, M. Kumjian, L. D. Carey, and W. A. Petersen, 2012: Use of dual polarization signatures in diagnosing tornadic potential. *Electronic J. Operational Meteor., Electronic J. Operational Meteor.*, **13** (5), 57-78.

———, W. A. Petersen, L. D. Carey, and D. J. Cecil, 2010: A dual-polarization investigation of tornado-warned cells associated with Hurricane Rita (2005). *Electronic J. Operational Meteor.*, **11** (4), 1–25

Crum, T. D., and R. L. Alberty, 1993: The WSR-88D and the WSR-88D Operational Support Facility. *Bull. Amer. Meteor. Soc.*, **74**, 1669–1687. doi: 10.1175/1520-0477(1993)074<1669:TWATWO>2.0.CO;2

Doviak, R. J., V. Bringi, A. Ryzhkov, A. Zahrai, and D. Zrnić, 2000: Considerations for polarimetric upgrades to operational WSR-88D radars. *J. Atmos. Oceanic Technol.*, **17**, 257–278.

Jedlovec, G. J., U. Nair, and S. L. Haines, 2006: Detection of storm damage tracks with EOS data. *Wea. Forecasting*, **21**, 249–267. doi: 10.1175/WAF923.1

Johnson, N., 2011: Debris times three: Conventional, Doppler, and polarimetric observations of a deadly 16 April 2011 tornado. *39th AMS Conference on Broadcast Meteorology and Conference on Weather Warnings and Communication*, Oklahoma City, OK.

King, M. D., Y. J. Kaufman, W. P. Menzel, and D. Tandré, 1992: Remote sensing of cloud, aerosol, and water vapor properties from the Moderate Resolution Imaging Spectrometer (MODIS). *IEEE Trans. Remote Sensing*, **30**, 2-27.

Klockow, K. E., R. McPherson, A. Tarhule, H. Brooks, and R. P. Thomas, 2012: How forecast and warning information, did, and did not, shape response in the April 27, 2011 tornado outbreak. *92nd AMS Annual Meeting*, New Orleans, LA.

Kumjian, M. R., 2011: Precipitation properties of supercell hook echoes. *Electronic J. Severe Storms Meteor.*, **6** (5), 1–21.

———, and A. V. Ryzhkov, 2008: Polarimetric signatures in supercell thunderstorms. *J. Appl. Meteor. Climatol.*, **47**, 1940–1961. doi: 10.1175/2007JAMC1874.1

Lemon, L. R., C. A. Van Den Broeke, C. Payne, and P. T. Schlatter, 2011: Dual polarimetric Doppler radar debris signature characteristics of a long-track EF-5 tornado. *36th Annual NWA Conference*, Birmingham, AL.

Molthan, A. L., G. J. Jedlovec, and B. C. Carcione, 2011: NASA satellite data assist in tornado damage assessments. *EOS*, **92**, No. 40, p. 337-339.

Palmer, R. D., and Coauthors, 2011: Observations of the 10 May 2010 tornado outbreak using OU-PRIME: Potential for new science with high-resolution polarimetric radar. *Bull. Amer. Meteor. Soc.*, **92**, 871–891. doi: http://dx.doi.org/10.1175/2011BAMS3125.1

Picca, J., and A. Ryzhkov, 2012: A dual-wavelength polarimetric analysis of the 16 May 2010 Oklahoma City extreme hailstorm. *Mon. Wea. Rev.*, **140**, 1385–1403.

Petersen, W. A., K. R. Knupp, D. J. Cecil, and J. R. Mecikalski, 2007: The University of Alabama Huntsville THOR Center instrumentation: Research and operational collaboration. 33rd Intl. Conf. on Radar Meteor., Amer. Meteor. Soc., Cairns, Australia, August 6-10, 2007.

———, L. D. Carey, K. R. Knupp, C. J. Schultz, and E. V. Johnson, 2008: ARMOR dual-polarimetric radar observations of tornadic debris signatures. *24th Conf. on Severe Local Storms*, Savannah, GA, Amer. Met. Soc.

Ryzhkov, A. V., T. J. Schuur, D. W. Burgess, and D. S. Zrnić, 2005: Polarimetric tornado detection. *J. Appl. Meteor.*, **44**, 557–570. doi: 10.1175/JAM2235.1

Scharfenberg, K. A., and Coauthors, 2005: The Joint Polarization Experiment: Polarimetric radar in forecasting and warning decision making. *Wea. Forecasting*, **20**, 775–788. doi: 10.1175/WAF881.1

Schultz, C. J., and Coauthors, 2011: The use of dual polarimetric tornadic debris signatures in an operational setting. *36th Annual NWA Conference*, Birmingham, AL, Natl. Wea. Assoc.

———, and Coauthors, 2012: Dual-polarization tornadic debris signatures Part I: Examples and utility in an operational setting. *Electronic J. Operational Meteor.*, **13** (9), 120-137.

Schlatter, P. 2012: Dual-polarization radar tornadic vortex signature best practices. *37th Annual NWA Conference*, Madison, WI, Natl. Wea. Assoc. E11.2

Snyder, J. C., H. B. Bluestein, G. Zhang, and S. J. Frasier, 2010: Attenuation correction and hydrometeor classification of high-resolution, X-band, dual-polarized mobile radar measurements in severe convective storms. *J. Atmos. Oceanic Technol.*, **27**, 1979–2001. doi: http://dx.doi.org/10.1175/2010JTECHA1356.1

Tabary, P., F. Vulpiani, J. J. Gourley, A. J. Illingworth, R. J. Thompson, and O. Bousquet, 2009: Unusually high differential attenuation at C-band: Results from a two-year analysis of the French Trappes polarimetric radar data. *J. Appl. Meteor. Clim.*, **48**, 2037-2053.

Tanamachi, R. L., H. B. Bluestein, J. B. Houser, S. J. Fraiser, and K. M. Hardwick, 2012: Mobile, X-band polarimetric Doppler radar observations of the 4 May 2007 Greensburg, Kansas tornadic supercell. *Mon. Wea. Rev.*, accepted, in press.

Warning Decision Training Branch, 2011: Dual-pol Applications. [http://www.wdtb.noaa.gov/courses/dualpol/index.html]